Int. J. Pure Appl. Sci. Technol., 30(1) (2015), pp. 29-42

International Journal of Pure and Applied Sciences and Technology

ISSN 2229 - 6107

Available online at ***www.ijopaasat.in***

Research Paper

Incidence Angle Effect on Electrical Parameters of a Bifacial Silicon Solar Cell Illuminated by its Rear Side in Frequency Domain

Amary Thiam[1], Gokhan Sahin[1], Mohamed Abderrahim Ould El Moujtaba[1], Babacar Mbow[1], Marcel Sitor Diouf[1], Moussa Ibra Ngom[1] and Grégoire Sissoko[1,*]

[1] Department of Physics, Faculty of Sciences and Techniques, University of Cheikh Anta Diop, Dakar, Senegal

* Corresponding author, e-mail: (gsissoko@yahoo.com)

(Received: 4-8-15; Accepted: 29-9-15)

Abstract: *The dynamic impedance $Z(\omega,\theta)$ of bifacial Silicon solar cell under incidence angle, obtained by the ratio of the photocurrent density $J_{Ph}(\omega,\theta)$ to the photovoltage $V_{Ph}(\omega,\theta)$, is studied by use of Nyquist and Bode diagrams in order to determine electrical parameters.*

Keywords: Bifacial solar cell, Frequency modulation, Incidence angle, Recombination velocity.

1. Introduction

In order to improve efficiency, many studies are made on n^+-p-p^+ silicon solar cell type (Daniel L. Meier et al, 1998; A. Hübner et al, 2001). The knowledge of the intrinsic and extrinsic phenomena of semiconductors is fundamental for the manufacturing and operating the solar cells. In this work, a bifacial silicon solar cell is studied under different incidence angle values of a constant multispectral light in angular frequency modulation. After solving the continuity equation and considerating boundary conditions, we obtain the expression the minority carriers density which allows us to determine the photocurrent density $J_{Ph}(\omega,\theta)$ in frequency domain (K. Bouzidi et al, 2007; I.F. Barro et al, 2001; Nd. Thiam, 2012). From the photocurrent, the short-circuit photocurrent $J_{sc}(\omega,\theta)$ is established. Using the Boltzmann relationship, expressions of the photovoltage $V_{Ph}(\omega,\theta)$ and the open circuit photovoltage $V_{OC}(\omega,\theta)$, are obtained as a function of the frequency modulation and the

incidence angle light. The plots the photocurrent density module and photovoltage versus the logarithm of the angular frequency have two zones:

The first corresponding to the short-circuit operating the solar cell and the second to the open circuit operating. These expressions the photocurrent and photovoltage will allow us to get the dynamic impedance for different values the incidence angle the light by using the Nyquist and Bode diagrams (L. Bousse et al, 1994; A. Thiam et al, 2013). A study the space charge region capacitance for different values of the incidence angle, versus the logarithm the frequency, is done.

2. Theory

We use in this study, a monocrystalline bifacial silicon solar cell under constant multispectral illumination by its rear face. We present, in Figure (1), the n^+-p-p^+ solar cell type:

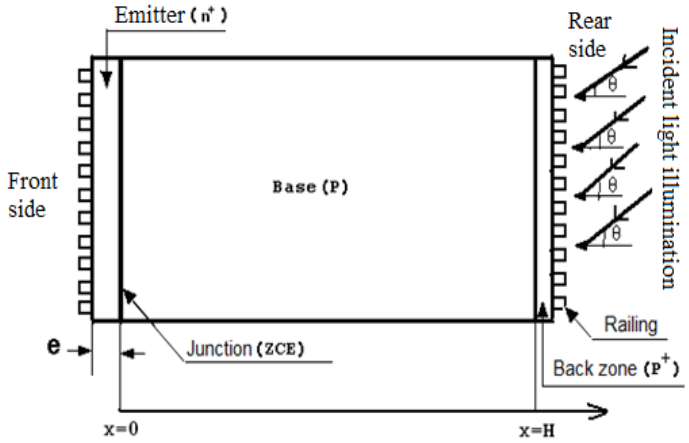

Figure 1: Bifacial solar cell under constant multispectral illumination on its back side

2.1 Continuity Equation

When we illuminate the rear side of a solar cell in frequency domain, the density of photo generated minority carriers in the base, is governed by the following continuity equation:

$$D(\omega).\frac{\partial^2 \delta(\omega,x,\theta,t)}{\partial x^2} - \frac{\delta(\omega,x,\theta,t)}{\tau} = -G(\omega,x,\theta,t) + \frac{\partial \delta(\omega,x,\theta,t)}{\partial t} \quad (1)$$

Where:

- $D(\omega)$ is the complex diffusion coefficient, which depends on the angular frequency,
- τ represents the average lifetime the minority carriers,
- t is the time
- $\omega = 2\pi f$ is the angular frequency and f the frequency,
- $\delta(\omega,x,\theta,t)$ represents the minority carriers density according to the time t, incidence angle θ, base depth x and angular frequency.
- $G(\omega,x,\theta,t)$ represents the overall generation rate of the minority carriers density and it can be expressed as follow (Noriaki Honma et al, 1988; Andreas Mandelis, 1989; G.Sissoko et al, 1998).

$$\delta(\omega, x, \theta, t) = \delta(x, \theta) \cdot \exp(j \cdot \omega \cdot t) \quad (2)$$

$$G(\omega, x, \theta, t) = g(x, \theta) \cdot \exp(j \cdot \omega \cdot t) \quad (3)$$

Where:

- j is the imaginary number $\left(j^2 = -1\right)$

- $\delta(x, \theta)$ denotes the spatial part of the density of generated carriers in the base depth x and $\exp(j.\omega.t)$ represents the time dependent of the density of charge carriers,

- $g(x, \theta)$ is the spatial part called generation rate depending on the depth the base for illumination from the back side of the solar cell and $\exp(j\omega.t)$ is the temporal part the overall rate generation $G(\omega, x, \theta, t)$.

$$g(x, \theta) = n \cdot \cos\theta \cdot \sum_{k=1}^{3} a_k \cdot \exp - b_k (H - x) \quad (4)$$

- n is the number of sun;

a_k and b_k : are coefficients (G. Sissoko et al, 1996; K. Misiakos, 1990**)** defined under AM 1.5

Substituting the equations (2) and (3) to the equation (1), we obtain:

$$\frac{\partial^2 \delta(x, \theta)}{\partial x^2} - \frac{\delta(x, \theta)}{L(\omega)^2} = -\frac{g(x, \theta)}{D(\omega)} \quad (5)$$

Where:

$$L(\omega)^2 = \frac{L_0^2}{(1 + j\omega \cdot \tau)} \quad (6)$$

With $L(\omega) = \sqrt{D(\omega) \cdot \tau}$: is the complex diffusion length (Andreas Mandelis, 1989; G. Sissoko et al, 1998). A solution of the equation (5) can be expressed as:

$$\delta(x, \theta) = Ach\left(\frac{x}{L(\omega)}\right) + Bsh\left(\frac{x}{L(\omega)}\right) + \sum_{k=1}^{3} \beta_k \exp\left(- b_k (H - x)\right) \quad (7)$$

With

$$\beta_k = \frac{L(\omega)^2 \cdot n \cdot \cos(\theta)}{D(\omega) \cdot \left(1 - L(\omega)^2 \cdot b_k^2\right)} \cdot a_k \quad (8)$$

and $D(\omega)(1 - b^2 L(\omega)^2) \neq 0$

The coefficients A and B are given by the boundary conditions:

❖ At the junction $(x = 0)$

$$D(\omega) \cdot \left. \frac{\partial \delta(x,\theta)}{\partial x} \right|_{x=0} = Sf \cdot \delta(x,\theta)\big|_{x=0} \qquad (9)$$

❖ At the rear side $(x = H)$

$$D(\omega) \cdot \left. \frac{\partial \delta(x,\theta)}{\partial x} \right|_{x=H} = -Sb \cdot \delta(x,\theta)\big|_{x=H} \qquad (10)$$

Where Sf and Sb are the recombination velocities at the junction and the rear side respectively (F.I.BARRO and A. Seidou MAIGA, 2010; J. Dugas, 1994);

H is the thickness of the bifacial photovoltaic cell.

After calculating all the phenomenological and electrical parameters can be set in complex notation (A. Dieng et al, 2011); thereafter, the study is carried out only on the modules complex quantities.
In figure (2) we present the module the minority carriers density profile versus base depth:

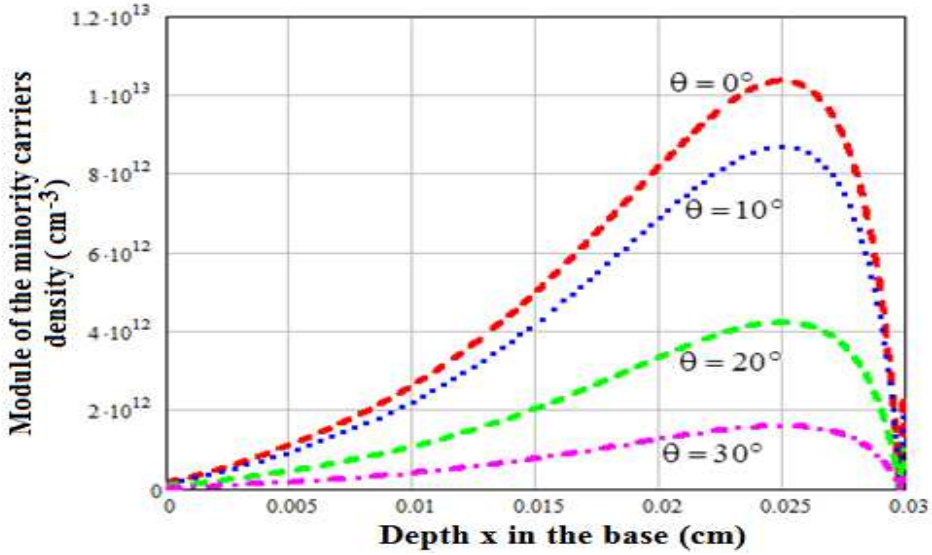

Figure 2: Module of the minority carriers density versus the base depth, for different values of incidence angles in rear side illumination

$\omega = 8.10^5 \text{ rad/s}$, $Sf = 3.10^3 cm/s$, $H = 0.03\text{cm}$, $L_0 = 0.02cm$, $D_0 = 35cm^2.s^{-1}$, $\tau = 1.10^{-5}s$

The carrier density increases with depth x, the junction to a maximum value located to the rear side of the base. In that base region, the gradient of the carriers being positive, then the minority carriers located in this region may cross the junction and generate a photocurrent. The maximum density corresponds to a nil gradient of minority carriers. Then this density decreases with depth x in the base. In this area, the carriers can not cross the junction for producing a photocurrent. They will recombine. It is noted that the greater the angle of incidence increases, the module of the density carriers decreases. The variation of the density minority carriers in the base depending on the depth x and the incidence angle light, causes the appearance photocurrent to the terminals of the bifacial solar cell.

2.2 Photocurrent

The photocurrent is obtained by the gradient minority carriers through the junction and is given by:

$$J_{Ph} = e \cdot D(\omega) \cdot \frac{\partial \delta(x,\theta)}{\partial x}\Big|_{x=0} \qquad (11)$$

Where, **e** is the elementary charge of electron.

This photocurrent density can be written in complex form. The module of the photocurrent density, for different incidence angle, versus junction recombination velocity, is represented in figure 3:

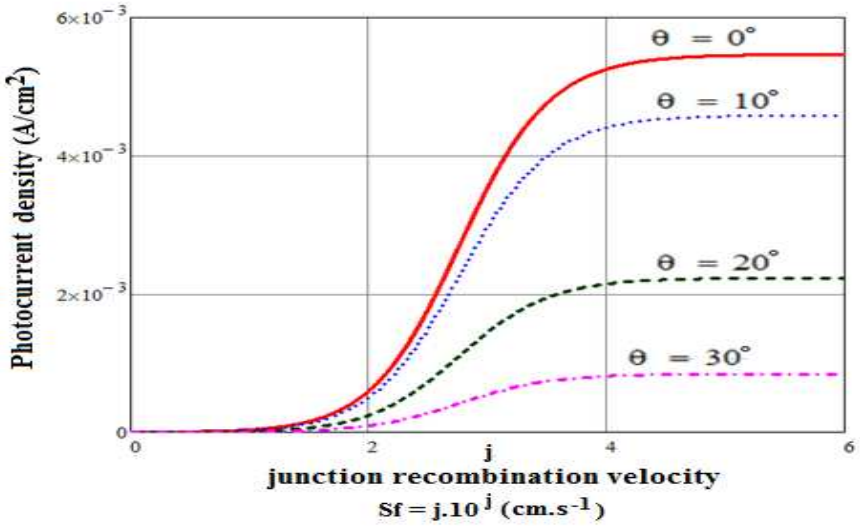

Figure 3: Module of the photocurrent density versus the junction recombination velocity for different values of incidence angles in rear side illumination

$H = 0.03\text{cm}\,; L_0 = 0.02cm\,; D_0 = 35cm^2/s\,; \tau = 1.10^{-5}s\,,\ \omega = 10^5 \text{ rad/s}$

For a given incidence angle, the photocurrent density increases for various junction recombination velocity. Its profile presents three zones:

i) The first corresponds to the open circuit operating the solar cell in the interval [0 $cm.s^{-1}$; $2.10^2 cm.s^{-1}$];

ii) The second, to the interval [2.10^2 $cm.s^{-1}$; $4.10^4 cm.s^{-1}$] where the photocurrent varies with the operating point of the solar cell;

iii) The third, to the interval [4.10^4 $cm.s^{-1}$; $7.10^7 cm.s^{-1}$] where the photocurrent is equal to short circuit photocurrent the solar cell. We note that, increasing incidence angle leads to a decrease the photocurrent amplitude since there is no more significant photo generated carriers that crossed the junction edge.

2.2.1 Short-Circuit Photocurrent

The expression the photocurrent allows us to obtain the short circuit photocurrent. Its profile is represented in Figure 4.

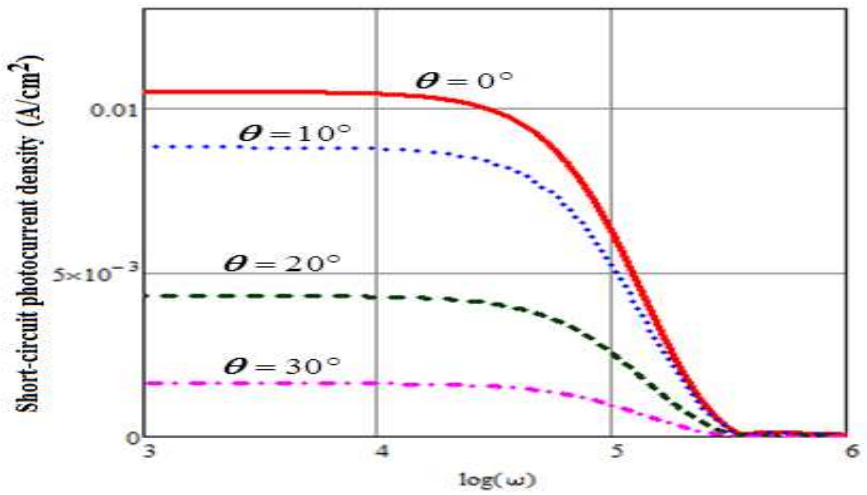

Figure 4: Module of the short-circuit photocurrent versus the logarithm of angular frequency for different values of incidence angles of the light in rear side illumination

$H = 0.03\text{cm}\,;\, L_0 = 0.02cm\,;\, D_0 = 35cm^2.s^{-1}\,;\, \tau = 1.10^{-5}s$

Figure4 shows that the short-circuit current the module picture shows a plateau for frequencies low values then decreases for superior frequency $1.78.10^5$ Hz. This module the photocurrent density also decreases as a function of the angle of incidence of light.

At the end of this study on the photocurrent, we will determine the photovoltage as a function of the incidence angles, the recombination rate and the logarithm of the frequency.

2.3 Photovoltage

The expression of the photovoltage can be obtained from the Boltzmann relation below:

$$V_{Ph} = V_T \cdot \ln\left(1 + \frac{N_b}{n_0^2} \cdot \delta(0)\right) \qquad (12)$$

$$V_T = \frac{k.T}{e}$$

In this equation

V_T is the thermal voltage

k is the Boltzmann constant

T is the absolute temperature at thermal equilibrium (300K)

N_b is the doping rate the base impurity atoms

n_0 is the intrinsic carrier concentration.

Its profile is given in figure 5 below:

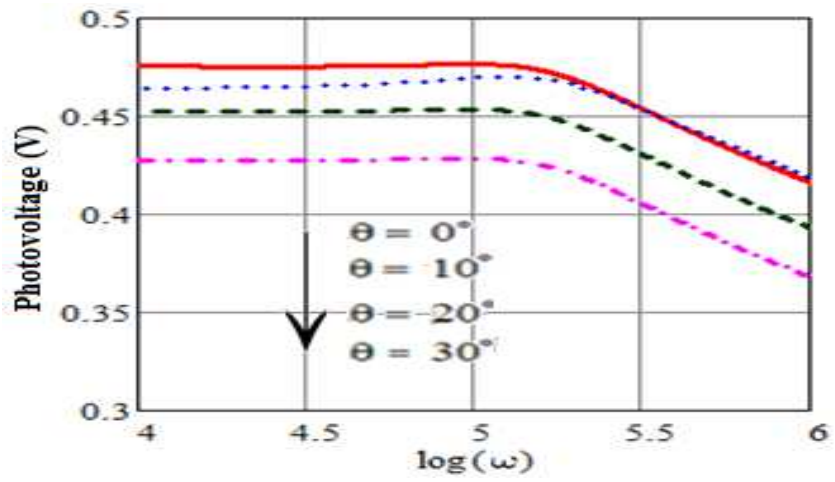

Figure 5: Module of the photovoltage versus the logarithm of frequency for different values of incidence angles in rear side illumination

$H = 0.03\text{cm}, L_0 = 0.02cm, D_0 = 35cm^2/s, \tau = 1.10^{-5}s$

The photovoltage has a horizontal bearing for low frequency values corresponding to the open circuit voltage, then decreases for high frequencies. The module the photovoltage decreases if the angle incidence of the light increases.

Subsequently we will study the open circuit photovoltage versus the logarithm frequency for different values of incidence angles.

2.3.1 Open Circuit Photovoltage

One can get the open circuit photovoltage from equation (11). The module of the open circuit photovoltage, depending on the angular frequency and the light incidence angle, is represented in Figure 6:

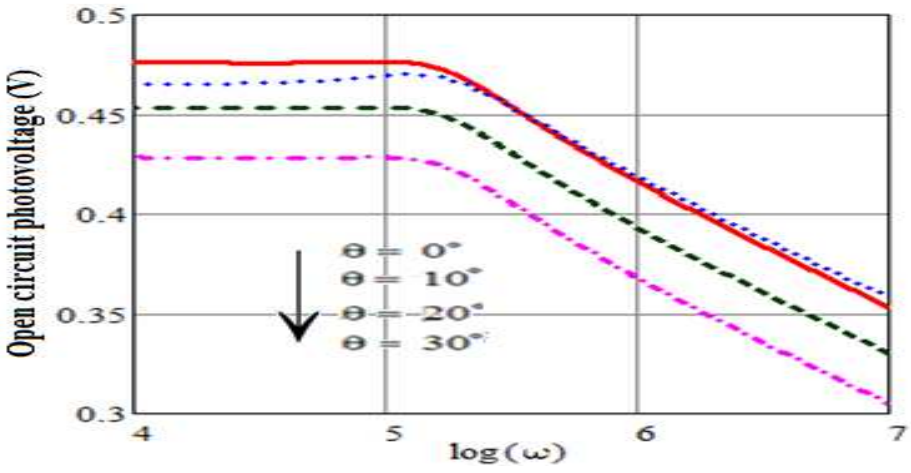

Figure 6: Open circuit photovoltage module versus the angular frequency different incidence angles

$H = 0.03\text{cm}; L_0 = 0.02cm; D_0 = 35cm^2.s^{-1}; \tau = 1.10^{-5}s$

The storage photogenerated carriers at the vicinity the junction is more important for low frequency values, in quasi-steady state. For high angular frequencies in the interval [10^5 rad.s^{-1}; 10^7 rad.s^{-1}] the open-circuit photovoltage decreases.

An increase of the incidence angle leads to a decrease of the open circuit photovoltage module since there is a feeble absorption of the incident photons by the sample.

4. The Impedance Phase

The expression of the impedance is given by:

$$\varphi(\omega,\theta) = \arg\left(Z(\omega,\theta)\right) \qquad (13)$$

The profile this phase versus the logarithm of the angular frequency, for different incidence angles, is represented in figure 7:

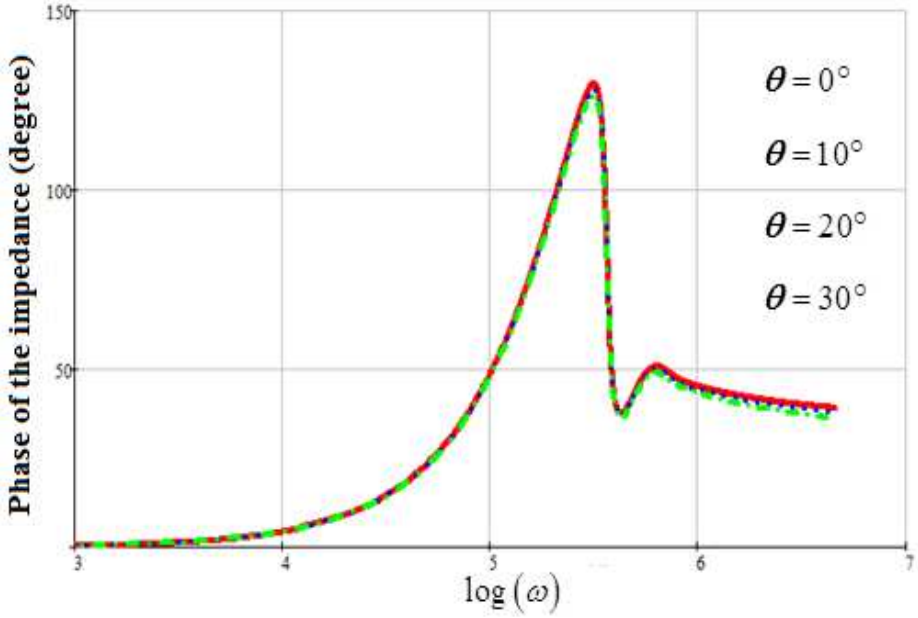

Figure 7: Impedance phase versus the logarithm of the angular frequency for different incidence angle values

$H = 0.03\text{cm}\,; L_0 = 0.02cm\,; D_0 = 35cm^2.s^{-1}\,; \tau = 1.10^{-5}s$

We observe in figure 7 that the phase of the impedance is steel positive with angular frequency, and independent of the incidence angle of the light. This behavior of the phase confirms that the solar cell impedance can be considered as a self – inductance in parallel with a resistance.

5. NYQUIST Diagram

The NYQUIST diagram (Pannalal L.B, 1973-1974) consists on representing an imaginary part versus a real part of a complex function. Here, we give the dynamic impedance expression in equation13.

$$Z(\omega,\theta) = \frac{V_{Ph}(\omega,\theta)}{J_{ph}(\omega,\theta)} \qquad (14)$$

And its imaginary part versus its real part, is represented in figure7:

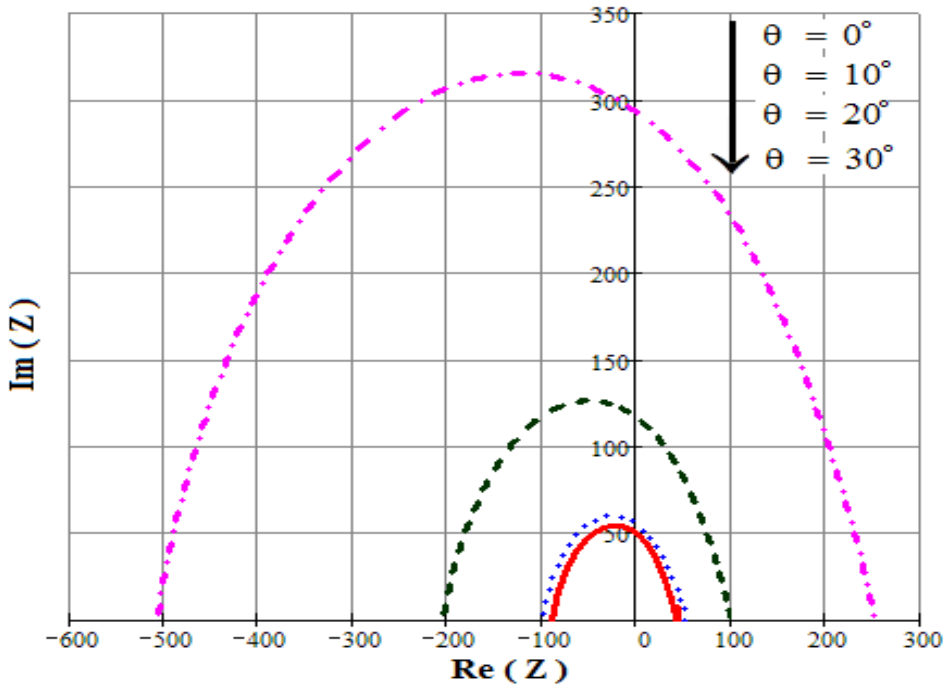

Figure 8: The imaginary part of the dynamic impedance versus its real part for different values of the incidence angles of the light

$H = 0.03\text{cm}\,; L_0 = 0.02cm\,; D_0 = 35cm^2.s^{-1}\,; \tau = 1.10^{-5}s$

We note that the obtained curves increase in diameter if the incidence angle increases. These curves are semicircles of radius $\left(\frac{Rp}{2}\right)$. Where R_p represents the semicircle diameter.

The analysis of the curves in figure 7 shows that for frequencies near to the cutoff frequency, the imaginary part is equal to $\left(\frac{R_p}{2}\right)$ and the real part is equal $\left(\frac{R_p}{2}+R_S\right)$; this point corresponds to the maxima the curves.

For the determination the electrical parameters, we consider different curves presented, for different incidence angle values in figure 9:

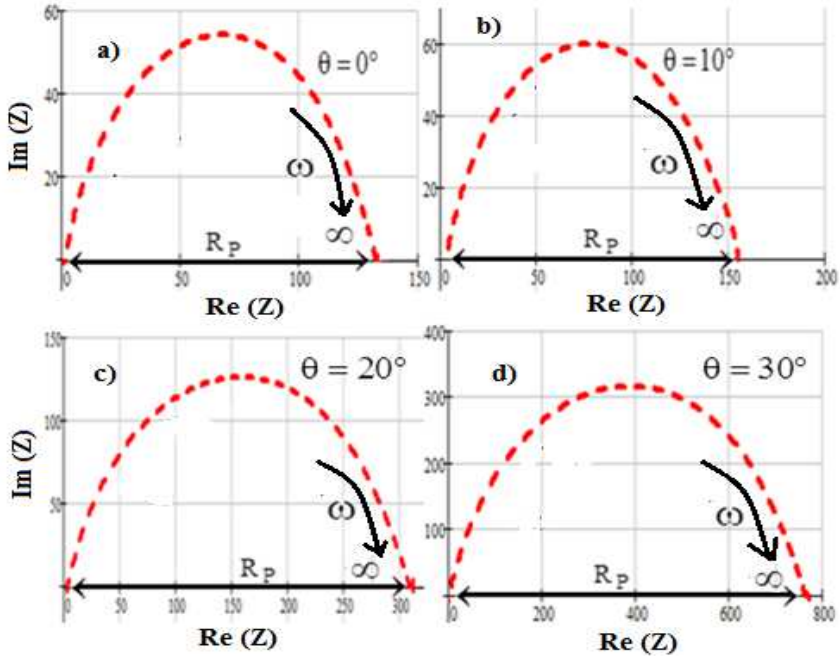

Figure 9: Imaginary part versus the real part of the impedance for different incidence angle values
$H = 0.03\text{cm}\,; L_0 = 0.02cm\,; D_0 = 35cm^2/s\,\,; \tau = 1.10^{-5}s$

Illumination by the rear side reveals that the inductive effect is predominant to the capacitive effect. Thus, the photovoltaic cell can be modeled as a resistor R_P in parallel with a self-inductance.
In table1, we give, for different incidence angles, a few series resistance and parallel resistance.

Table 1: Light incidence angle effect on photovoltaic cell series and parallel resistances

θ (°)	0	10	20	30
Rs $(\Omega.\text{cm}^2)$	0,082	0,103	0,212	0,582
Rp $(\Omega.\text{cm}^2)$	133,1	152,30	309,40	769,10

The table above shows that when the incidence angle of the light increases, the series resistance as the parallel resistance also increase that involves a poor conduction the photocurrent. Therefore, an increase in the incidence angle of the illumination leads to an increase the leakage current and the ohmic losses the bifacial photovoltaic cell.

6. Series Resistance

The series resistance characterizes the resistive effects of material and the device of used contact. Expression the series resistor (Amadou Diao et al, 2014) is given by Equation 15:

$$R_S(\omega,\theta,Sf) = \frac{V_{oc}(\omega,\theta) - V_{Ph}(\omega,\theta,Sf)}{J_{Ph}(\omega,\theta,Sf)} \qquad (15)$$

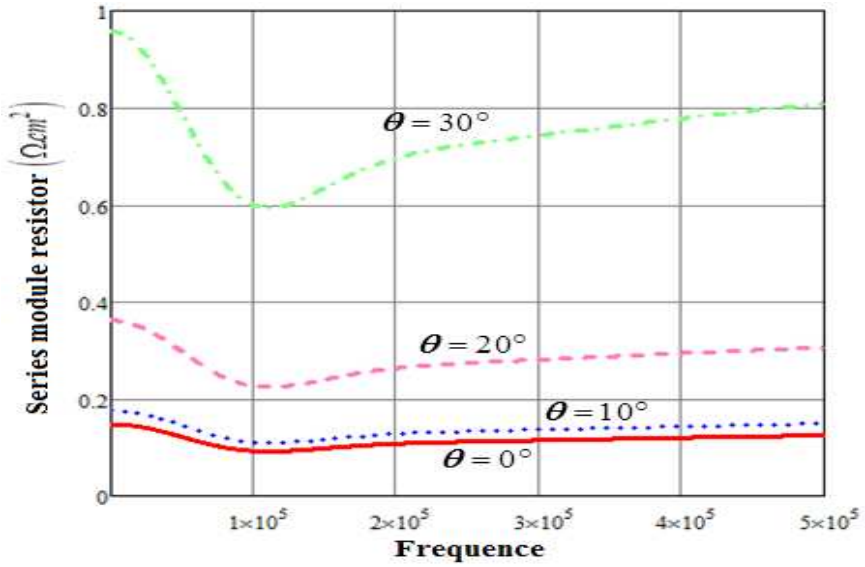

Figure 10: Module of series resistance versus angular frequency for different incidence angles:
H = 0.03cm ; $L_0 = 0.02cm$; $D_0 = 35cm^2 / s$; $\tau = 1.10^{-5} s$

Figure10 shows that for small values the frequency in steady state the series resistance is low, and constant for a given incidence angle value. When switching to higher frequencies, the series resistance increases rapidly, so the photogenerated carriers cannot participate into the photocurrent. The increase of the incidence angle of the light, corresponds to an increase the series resistance amplitude, which indicates an ohmic solar cell. This is in agreement with the results found in Table1.

7. BODE Diagram

The BODE diagram is a method developed to simplify the frequency response plots (A. Dieng et al, 2007). The module of the dynamic impedance versus the logarithm of the angular frequency, for different incidence angle values, is given in Figure 11.

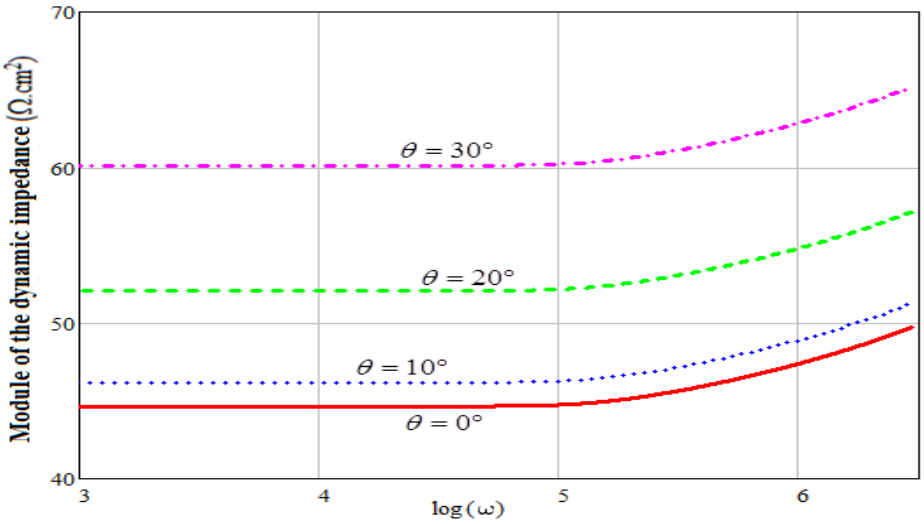

Figure 11: Module dynamic impedances versus the logarithm of the frequency under different incidence angle values
H = 0.03cm ; $L_0 = 0.02cm$; $D_0 = 35cm^2 / s$; $\tau = 1.10^{-5} s$

In figure11, the dynamic impedance increases with the logarithm of the angular frequency for a given incidence angle. We note that the cut – off frequency is not affected by the incidence angle. In figure12, we present a method to determine the cut – off frequency:

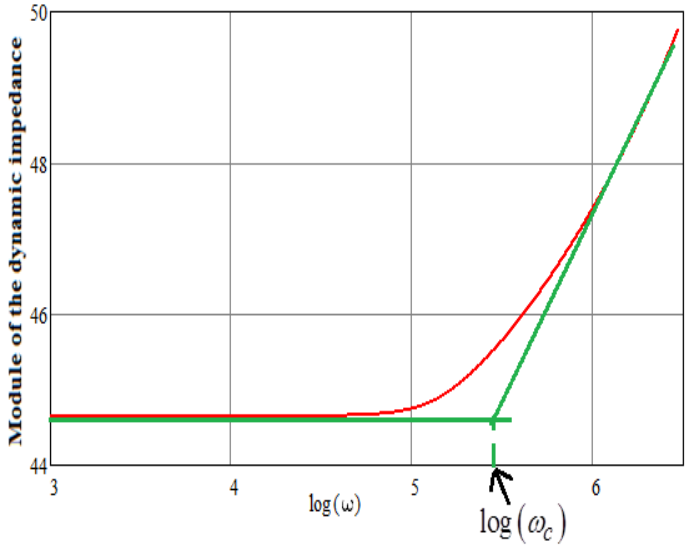

Figure 12: Module of dynamic impedances versus the logarithm of the frequency (knee point)
$H = 0.03cm\,; L_0 = 0.02cm\,; D_0 = 35cm^2.s^{-1}\,; \tau = 1.10^{-5}s$

The intercepted point obtained by the two tangent lines curves, projected on the $\log(\omega)$ axis, corresponds to the $\log\omega_c$ from which the cut – off angular frequency ω_C is determined; its value is:

$$\omega_c = 1,2.10^5 rad.s^{-1}$$

A relation between parameters R_p, C and ω_C, is given by equation (16):

$$R_P \cdot C = \frac{1}{\omega_c} \qquad (16)$$

The expression of the capacitance at the cut – off frequency is as following

$$C = \frac{1}{\omega_c \cdot R_p} \qquad (17)$$

From this equation we give in Table (2) a few values capacitance depending on the incidence angle of light.

Table 2: Capacitance for different incidence angle values of the illumination

θ (°)	0	10	20	30
$C\left(\mu F.cm^{-2}\right)$	0,028	0,025	0,012	0,005

It is noted that the capacitance decreases when the incidence angle increases.

8. Junction Capacitance

At the junction, we define a capacitance (M.M. Deme et al, 2010) whose expression is given by equation 18:

$$C = \frac{q^2}{K \cdot T}\left(\frac{n_0^2}{N_b} + \delta(0)\right) \qquad (18)$$

The profile this capacitance versus the logarithm of the angular frequency is given in figure 13:

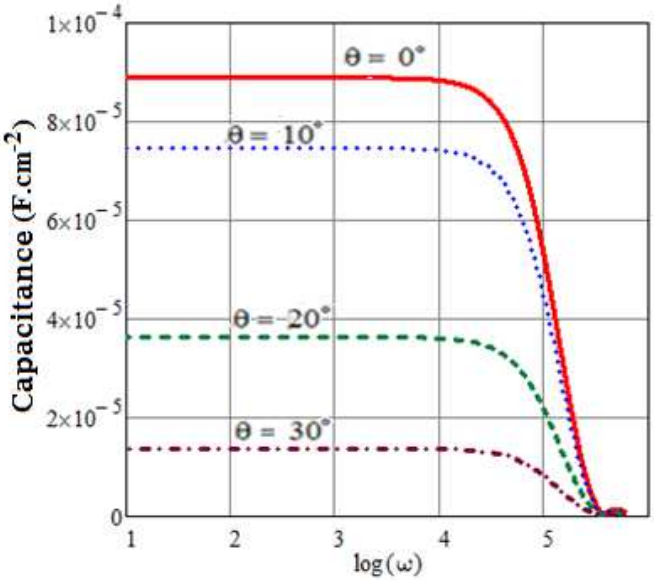

Figure 13: Module of capacitance versus logarithm of angular frequency for different values of the incidence angle: $H = 0.03\text{cm}\,; L_0 = 0.02cm\,; D_0 = 35cm^2.s^{-1}\,; \tau = 1.10^{-5}s$

For a given incidence angle value, the capacitance is constant in quasi – steady state but in the frequency domain, we note a decrease the capacitance since there is no significant stored photogenerated minority carriers in the vicinity the junction. When we increase the incidence angle, there is a reduction the illuminated solar cell area: This fact causes an increase the reflection coefficient and a feeble absorption of the sample. Consequently, the amplitude of the capacitance decreases.

Conclusion

A theoretical study on the density minority carriers in the base a bifacial silicon solar cell has been done. The expressions the photocurrent and photovoltage are established according to the angular frequency modulation and different incidence angles. From the representation of Nyquist and Bode diagrams, we have determined a few electrical parameters the solar cell and understand the influence of the incidence angles these electrical parameters. We note degradation properties the solar cell when both angular frequencies and incidence angles increase.

References

[1] D.L. Meier, J.M. Hwang and R.B. Campbell, IEEE transactions on electron devices, ED-35(1) (1988), 70-78.

[2] A. Hübner, A.G. Aberle and R. Hezel, 20% Efficient bifacial silicon solar cells, *14th European PVSEC*, Munich, (2001), 1796-1798.

[3] K. Bouzidi, M. Chegaar and A. Bouhemadou, Solar cells parameters evaluation considering the series and shunt resistance, *Solar Energ. Mater. Solar Cells*, 91(2007), 1647-1651.

[4] I.F. Barro, I. Zerbo, O.H. Lemrabott, F. Zougmore and G. Sissoko, Bulk and surface recombination parameters measurement in silicon double sided surface field solar cell under constant white bias light, *Proc. 17th European PVSEC*, Munich, (2001), 368-371.

[5] N. Thiam, A. Diao, M. Ndiaye, A. Dieng, A. Thiam, M. Sarr, A.S. Maiga and G. Sissoko, Electric equivalent models of intrinsic recombination velocities of a bifacial silicon solar cell under frequency modulation and magnetic field effect, *Research Journal of Applied Sciences, Engineering and Technology*, 4(22) (2012), 4646-4655.

[6] L. Bousse, S. Mostarshed, D. Hafeman, M. Sartore, M. Adami et C. Nicolini, Investigation of carrier transport through silicon wafers by photocurrent measurements, *J. Appl. Phys.*, 75(8) (1994), 4000-4008.

[7] A. Thiam, M. Zoungrana, H. Ly Diallo, A Diao, N. Thiam, S. Gueye, M.M. Deme, M. Sarr and G. Sissoko, Influence of incidence illumination angle on capacitance of a silicon solar cell under frequency modulation, *Research Journal of Applied Sciences, Engineering and Technology*, 5(4) (2013), 1123-1128.

[8] N. Honma, C. Munakata and H. Shimizu, Calibration of minority carrier lifetime measured with an ac photovoltaic method, *Japanese Journal of Applied Physics*, 24(7) (1988), 1322-1326.

[9] A. Mandelis, Coupled ac photocurrent and photothermal reflectance response theory of semiconducting p-n junctions, *J. Appl. Phys.*, 66(11) (1989), 5572-5583.

[10] G. Sissoko, E. Nanéma, A.L. Ndiaye, Y.L.B. Bocandé and M. Adj, Minority carrier diffusion length measurement in silicon solar cell under constant white bias light, *Renewable Energy*, 3(1996), 1594-1597, Pergamon, 0960-1481/94$ 700 +0.00.

[11] G. Sissoko, C. Museruka, A. Corréa, I. Gaye and A.L. N'Diaye, Light spectral effect on recombination parameters of silicon solar cell, *Renewable Energy*, 3(1996), 1487-1490, Pergamon.

[12] K. Misiakos, C.H. Wang, A. Neugroschel and F.A. Lindholm, Simultaneous extraction of minority-carrier parameters in crystalline semiconductors by lateral photocurrent, *J. Appl. Phys.*, 67(1) (1990), 321-333.

[13] F.I. Barro, A.S. Maiga, A. Wereme and G. Sissoko, Determination of recombination parameters in the base of a bifacial silicon solar cell under constant multispectral light, *Phys. Chem. News*, 56(2010), 76-84.

[14] J. Dugas, 3D modelling of a reverse cell made with improved multicrystalline silicon wafers, *Solar Energy Materials and Solar Cell*, 32(1) (1994), 71-88.

[15] A. Dieng, N. Thiam, A. Thiam, A.S. Maiga and G. Sissoko, Magnetic field effect on the electrical parameters of a polycrystalline silicon solar cell, *Res. J. Appl. Sci. Eng. Technol.*, 3(7) (2011), 602-611.

[16] L.B. Pannalal, Signals, Systems and Controls, New York: Intext Educational, (2011), 1973-1974.

[17] A. Diao, N. Thiam, M. Zoungrana, G. Sahin, M. Ndiaye and G. Sissoko, Diffusion coefficient in silicon solar cell with applied magnetic field and under frequency: Electric equivalent circuits, *World Journal of Condensed Matter Physics*, 4(2014), 84-92.

[18] A. Dieng, L.O. Habiboulahy, A.S. Maiga, A. Diao and G. Sissoko, Impedance spectroscopy method applied to electrical parameters determination on bifacial silicon solar cell under magnetic field, *Journal des Sciences*, 7(3) (2007), 48-52.

[19] M.M. Deme, S. Mbodji, S. Ndoye, A. Thiam, A. Dieng, and G. Sissoko, Influence of illumination incidence angle, grain size and grain boundary recombination velocity on the facial solar cell diffusion capacitance, *Revues des Energ Renouvelab*, 13(1) (2010), 109-121.